Boron Catalysis in a Designer Enzyme

Lars Longwitz[1†], Reuben B. Leveson-Gower[1†], Henriëtte J. Rozeboom[2], Andy-Mark W. H. Thunnissen[2], Gerard Roelfes[1*]

[1]Stratingh Institute for Chemistry, University of Groningen, 9747, AG, Groningen, The Netherlands

[2]Groningen Biomolecular Sciences and Biotechnology Institute, University of Groningen, 9747, AG, Groningen, The Netherlands

Keywords: Designer enzymes, boron catalysis, non-canonical amino acids

One Sentence Summary: Genetically introducing boron into a designer enzyme unlocks an abiological activation mode which enables new-to-nature catalysis.

Abstract:

The creation of enzymes containing non-biological functionalities with activation modes outside of Nature's canon paves the way towards fully programmable biocatalysis. Here, we present a fully genetically encoded boronic acid containing designer enzyme with organocatalytic reactivity not achievable with natural or engineered biocatalysts. This boron enzyme catalyzes the kinetic resolution of hydroxyketones by oxime formation where crucial interactions with the protein scaffold assist in the catalysis. A directed evolution campaign lead to a variant with natural enzyme like enantioselectivities for a number of different substrates. The unique activation mode of the boron enzyme was studied via X-ray crystallography, high resolution mass spectrometry and ^{11}B NMR spectroscopy and opens up the possibility for a new class of boron dependent biocatalysts.

Boron can be considered an orphaned element since, while relatively abundant on earth, it remains unutilized by Nature's life creating machinery. It exclusively occurs in a stable oxygen bound form (*1*) and low valent organoboron compounds in particular are not used in nature. Conversely, these compounds are extremely important in modern organic chemistry as a means to construct carbon-carbon bonds (*2*), they find application as medicines (*3*) and can also be used as remarkably versatile catalysts. Boronic acids are particularly powerful catalysts due to their diverse substrate activation modes, including hydrogen bonding, anhydride formation, Lewis or Brønsted acid behavior as well as their selective binding to alcohols (*4-7*). For example, the activated achiral catalyst pentafluoro phenyl boronic acid (*8*) catalyzes amidations (*9, 10*), cyclo additions (*11, 12*), dehydrations (*13-15*) and many other reactions. However, there is only one example of a chiral catalyst that uses a boronic acid moiety as the catalytic center and other strategies rely on chiral thiourea (*16-21*) or amine (*22-26*) catalysts which are modified with a boronic acid to promote substrate-catalyst association (Figure 1A). Since an aryl substituent is required for boronic acid catalysis, inclusion of a vicinal chiral center is not possible, which stymies discovery of general approaches for asymmetric induction.

The design of a boronic acid dependent enzyme is a perfect avenue towards enantioselective boronic acid catalysis through directed evolution to improve selectivity and elaborate different reaction pathways by mutating the chiral protein environment (*27, 28*). By using stop codon suppression (SCS), boron can be genetically encoded in proteins as the non-canonical amino acid (ncAA) *para*-boronophenylalanine (pBoF) (*29*). This is an expedient route towards a boron enzyme, since it entails fully biosynthetic enzyme production (*30, 31*). SCS is a mature and readily applicable technology, and has been used to design enzymes which employ unnatural amino-groups (*32, 33*), nucleophiles (*34*) or photosensitizers (*35, 36*): activation strategies which are also found in Nature's biocatalysis toolbox (*37-39*) (Figure 1B). Herein, we demonstrate the full potential of ncAA based enzyme design, by using pBoF as a catalytic residue in an enzyme which operates by a xenobiotic mechanism that cannot be recreated using only natural proteogenic components. Our design exploits the affinity of boronic acids to vicinal diols, formed transiently after nucleophilic attack to carbonyls bearing a hydroxyl directing group, in order to catalyze a condensation reaction (Figure 1C). The boronic acid activates the substrate via covalent cyclic boronate ester formation rather than typical biocatalytic strategies of Lewis/Brønsted acid activation or utilizing oxyanion holes. We demonstrate that such an designer enzyme catalyzes the

stereoselective condensation of α-hydroxyketones with hydroxylamine to form oximes in a kinetic resolution, identify a highly selective evolved variant and provide insights into its unique boron dependent mechanism.

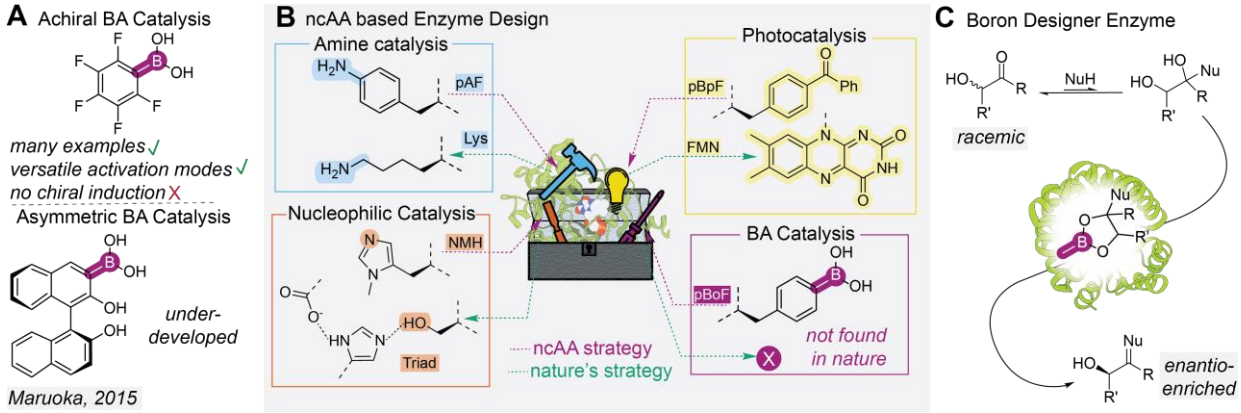

Figure 1. A. Achiral boronic acid (BA) catalysis is extremely versatile, however asymmetric variants are underdeveloped. **B.** ncAA based designer enzyme efforts to date have demonstrated the genetic encoding of amine catalysis, nucleophilic catalysis and photocatalysis, where similar strategies already exist in nature, except in the case of BA catalysis (this work). **C.** BA based designer enzymes provide a unique biocatalytic solution to the electrophilic activation of α-hydroxyketones.

Designer enzyme assembly and initial catalytic evaluation

Our initial efforts involved incorporation of pBoF into the dimeric Lactococcal multidrug resistance regulatory (LmrR) protein (*40*). Despite the fact that this transcriptional regulator lacks a natural catalytic function, it has a strong track record as a scaffold for designer enzymes as previously demonstrated by our group (Figure 2A) (*41*). We selected six positions (8, 11, 15, 89, 92 and 93) in the LmrR protein for pBoF incorporation, which are situated on helices α1 and α4, lining the hydrophobic cavity of the protein dimer interface, each providing a distinct chemical environment with potential to promote catalysis (Figure 2A). We targeted hydroxylamine as a convenient nucleophile to form a transient vicinal diol intermediate with an appropriate α-hydroxyketone, affording the corresponding oxime after boronic acid accelerated dehydration (*42*). In nature, biocatalysts for this reaction do not exist; instead, aldoxime containing natural products are formed via the oxidation of amines, not via nucleophilic substitution of the respective carbonyl (*43*). We selected racemic benzoin **(*Rac*)-1a** as an initial substrate and hypothesized that the protein environment would lead to the preferential conversion of one enantiomer leading to a kinetic resolution of the hydroxyl ketone (Figure 2B). We found that the condensation reaction between benzoin **1a** and hydroxylamine was accelerated in borate buffer, indicating that the dehydration reaction is facilitated by boron catalysis (*42, 44, 45*). Remarkably, every boron containing LmrR variant gave a significant yield of oxime products **(*E*)-2a** and **(*Z*)-2a** above the background and LmrR without pBoF, albeit without significant enantioselectivity in most cases (Figure 2C and SI.1). However, LmrR with pBoF incorporated at position 89 catalyzed the reaction with an E value (ratio between the catalytic rates for the two enantiomers) of 13, indicating considerable discrimination between substrate enantiomers by the resulting **b**oronic acid dependent **o**xime **s**ynthase (BOS from here on) (SI.2). Importantly, using the free amino acid pBoF or LmrR in which the pBoF residue was substituted with tyrosine (the closest natural structural analogue) completely abolished activity demonstrating a strong synergistic combination of the pBoF side chain in the LmrR scaffold for catalysis (SI.3).

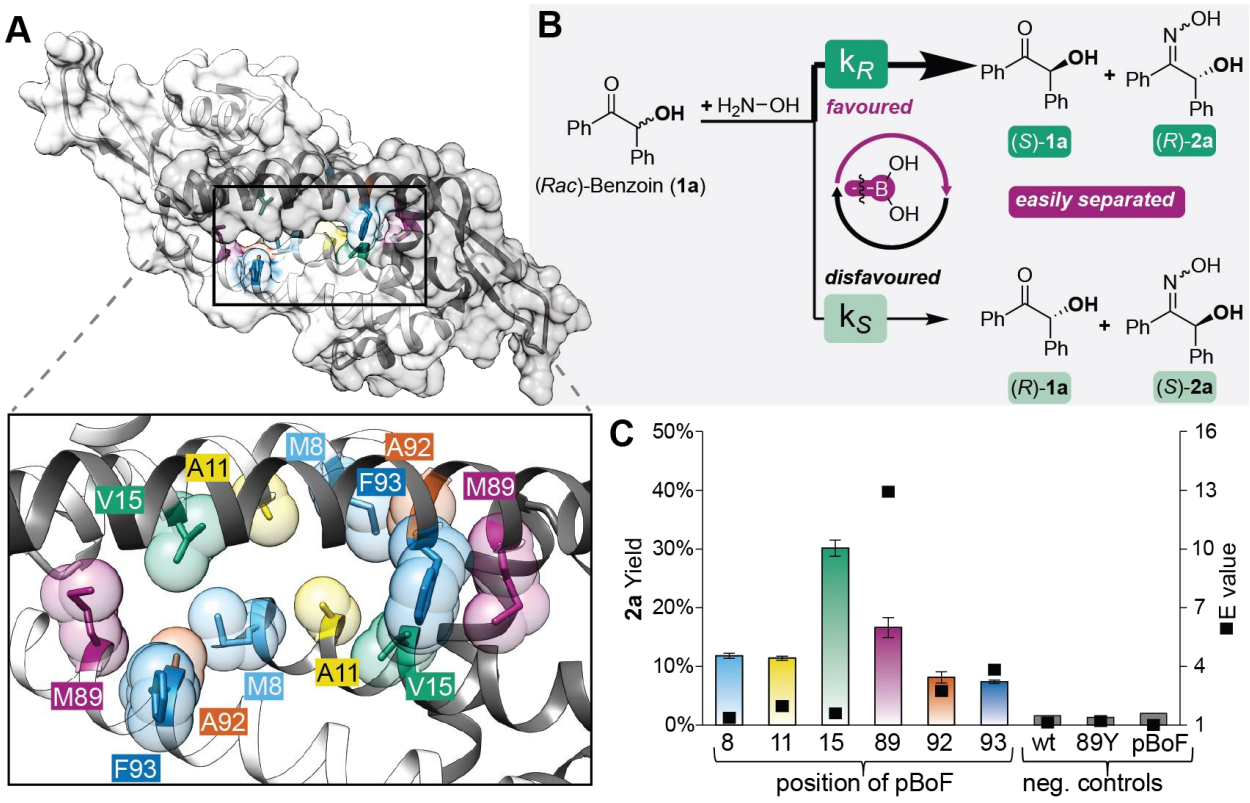

Figure 2. Assembly and evaluation of boronic acid functionalized designer enzymes in the kinetic resolution of benzoin **1a** via oximation. **A.** Overview of the homodimeric structure of LmrR (PDB: 3F8B) and enhanced view of the hydrophobic pocket showing selected positions for pBoF catalytic residue incorporation. **B.** Kinetic resolution of benzoin (**1a**) with hydroxylamine to form enantioenriched benzoin **1a** and benzoin oxime **2a**. **C.** Obtained yields and E values of benzoin oxime **2a** with different boron functionalized oxime synthases as well as negative controls. Reaction conditions (standard conditions): **(*Rac*)-1a** (1.0 mM), hydroxylamine (20 mM) and LmrR variant (25 µM dimer concentration) in buffer (20 mM Tris, 150 mM NaCl, pH = 8.0) with DMF (5.0 %v/v). Reactions conducted for 24 h at 4 °C and analyzed by normal-phase HPLC. The result obtained is an average of four experiments (two duplicates of two different batches of enzyme). All error values are given as standard deviations.

Directed evolution of the designer enzyme

Initial alanine scanning revealed a general mutability of BOS in various positions around the pBoF residue, without significant detriment to activity, setting a strong foundation for genetic optimization (SI.4). However, we found that the proximal residues N19 and K22 are crucial for catalytic activity as well as W96, which is key to LmrR's general structure (*46*). The mutant BOS_F93A already displayed a significant increase in catalytic activity and enantioselectivity. Notably, this mutant displayed sufficient catalytic activity to detect (*R*)-benzoin **(*R*)-1a** depletion via UV/Vis in cell-free lysates produced in 96-well plates, allowing us to proceed with a directed

evolution campaign (Figure 3A and SI.5). In the first round of evolution, site saturation mutagenesis (SSM) was performed at four positions (M8, L18, A92, F93) close to pBoF, identifying BOS_F93E as the best hit (SI.6). This variant afforded a 2.5-fold improved E value of 32 compared to BOS (E = 13) and was also more selective than the respective alanine mutant BOS_F93A (E = 21). Taking BOS_F93E as template we performed SSM at positions M8, V15, K22 and A92 (SI.7). In these libraries, mutants BOS_F93E_M8H and BOS_F93E_A92L were identified as hits, providing the major portion of their improvements in activity and selectivity, respectively. These second round mutations at the proximal residues produced a strong synergistic effect when combined to give BOS_F93E_M8H_A92L (henceforth BOS_EHL) which gives E values up to 146 (or 55 with only 1.0 mol% loading) and a 33-fold improvement in the observed rate constant (Figure 3B). These excellent selectivities are comparable to natural enzymes for their native substrates (*47*). The largest contribution to activity improvement in this mutant stems from the F93E mutation, which is responsible for a 9.5-fold increase. In combination, the M8H and A92L mutations give a 5.0-fold increase in E value, and a more modest 3.5-fold increase in activity. Regrettably, we could not characterize our variants using Michealis-Menten kinetics due to the generally low solubility of the benzoin derivatives **1** and the resulting low concentration of the intermediate hemiaminal (SI.8). When monitoring conversion of **(*Rac*)-1a** over time, the evolved variants show a massive loss in rate when approaching 50% conversion, having consumed their preferred substrate **(*R*)-1a** (Figure 3C). This effect is most prominent for the BOS_EHL variant, which also provides higher rate accelerations than a large excess (500-fold concentration) of simple borate. Interestingly, BOS_EHL preferentially forms the thermodynamically disfavored product *(Z)*-isomer, a preference which co-evolved with activity and enantioselectivity (SI.9). Based on the BOS_EHL template, six additional SSM libraries were generated and evaluated, however, no significantly improved variants were identified (SI.10). We continued with further examination of BOS_EHL. Whilst only one substrate, **1a**, was used for screening during the evolution campaign, the mutations in BOS_EHL bestow a general improvement in activity and selectivity across a range of substrates (Figure 3D and SI.11). Modification of the aromatic rings of the benzoin with methyl, methoxy or halogen substituents was well tolerated (**1b-1i**) and in many cases excellent selectivities (E > 100) were obtained. BOS_EHL even showed some activity and enantiomeric discrimination with strongly electron withdrawing groups like the ester **1j,** where no conversion was observed when using BOS.

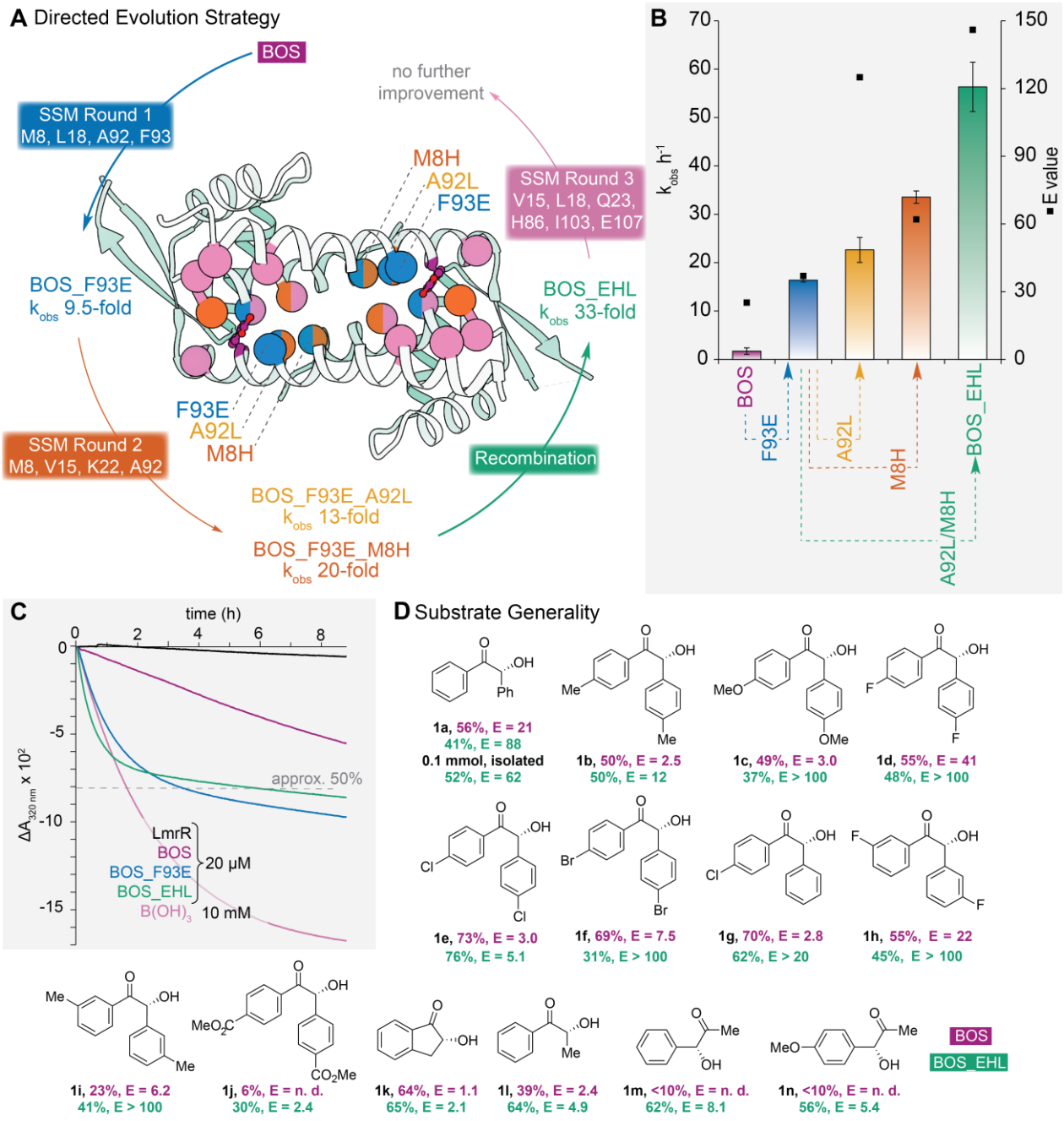

Figure 3. A. Trajectory of the directed evolution of BOS. **B.** Outcome of the evolution campaign on the observed rate constant for consumption of **(*R*)-1a** and the E values obtained with **(*Rac*)-1a** determined by HPLC (standard conditions with 50 µM BOS variant and 2 h reaction time). The result obtained is an average of four experiments (two duplicates of two different batches of enzyme). All error values are given as standard deviations. **C.** Time course measurements conducted with 0.5 mM **(*Rac*)-1a**. **D.** Substrate scope of the kinetic resolution of various hydroxyketones with BOS and BOS_EHL. Conversions and enantiomeric excess of remaining starting material is given. For reaction conditions, see SI.11.

Similarly, for the substrates **1k**, **1l** , **1m** and **1n** with greatly reduced steric-bulk around the chiral center only the improved mutant BOS_EHL showed satisfying conversion and selectivities. The necessity of the substrate to form a transient vicinal diol for the boron catalyzed mechanism was shown using acetylated benzoin and a β-hydroxyketone as control substrates, which were not converted (SI.11). To demonstrate the utility of our developed oximation procedure, a 500-fold upscale experiment was conducted with BOS_EHL, in which enantioenriched starting material (*S*)-benzoin **(*S*)-1a** as well as the product (*R*)-benzoin oxime **(*R*)-2a** were isolated in 52% and 37% yield, with enantiomeric excesses of 89% and 91%, respectively.

Evidence for the catalytic role of boronic acid

We sought to further validate the catalytic role of boron and study the influence of the protein environment on its activity. The established mechanism (*42, 44, 45*) of hydroxyl group directed boronic acid catalysis in water is comprised of three principle steps starting from the low-valent boronic acid resting state: (1) condensation of the transient vicinal diol substrate, formed from the spontaneous addition of hydroxyl amine to the ketone substrate, to generate an sp^3-hybridized cyclic boronate ester intermediate, (2) the rate determining dehydration to form a product-boronate condensate, and (3) hydrolytic product release (Figure 4, center). We conducted a series of analytic studies based on high resolution mass spectrometry (HRMS) (Figure 4A), ^{11}B NMR (Figure 4B) and X-ray crystallography (Figure 4C and 4D) to corroborate that these proposed boron species are formed in the BOS enzyme.

The boron center in BOS in the absence of substrate is indeed present in the low-valent boronic acid form as evidenced by HRMS showing the respective mass with partial dehydration under the ionization conditions, typical of boronic acid functionalized biomolecules (SI.12) (*48*). ^{11}B NMR spectroscopic analysis showed two major peaks at 23 ppm and 19 ppm, characteristic for low valent sp^2-hybridized boron species (Figure 4B) (*49-51*). The presence of two signals, which are in a pH dependent equilibrium (Figure 4B), could indicate that different protein conformers in solution influence the chemical shift or that weak Lewis acid/Lewis base adducts are formed with the boronic acid (SI.13 and SI.14). We obtained a 2.2 Å crystal structure of BOS at pH 6.0 which is also consistent with a sp^2-hybridized boronic acid state of the pBoF residues (Figure 4C).

The first step in catalysis involves the binding of vicinal diols to the boronic acid resting state which affords a sp^3-hybridized cyclic boronate ester intermediate. Since the proposed transient

vicinal diol substrate is present at concentrations undetectable by NMR, we characterized this binding process with several analogous, isolable vicinal diols (SI.15). The cyclic boronate ester intermediate is indeed formed almost quantitatively upon incubation of BOS with 4-nitrocatechol as observed with HRMS (Figure 4A), with an sp^3-hybridized state showing one characteristic sharp high-field shifted species at 8.6 ppm in its ^{11}B NMR spectrum (Figure 4B) (*51*). Similar results were also obtained with hydrobenzoin, which closely resembles the structure of the *in situ* formed reaction intermediate (Figure 4A and SI.16 and SI.17). Furthermore, BOS gave no boronate ester formation as observed by either ^{11}B NMR or HRMS upon addition of benzoin (**1a**), supporting its role as a precursor for the transient vicinal diol intermediate and not the substrate of a classical Lewis acidic carbonyl activation (SI.18). The product **2a** forms cyclic boronate ester species upon incubation with BOS, observed by ^{11}B NMR and HRMS, giving direct evidence for the last intermediate in the proposed catalytic cycle (Figure 4A and SI.16) (*51*). The evolved mutant BOS_EHL displays very similar substrate binding behavior in ^{11}B NMR spectroscopy and HRMS compared to the parent BOS, thus most likely follows the same mechanism (SI.10 and SI.20). The buffering compound Tris also partially forms a cyclic boronate ester species (Figure 4B and SI.21), however none of the tested binders caused catalysis inhibition, probably due to much faster on-off-rates than the turnover rate (Figure 4B and SI.22) (*52*). In contrast, simple aryl boronic acids did not show any formation of Tris adducts under identical conditions, indicating a strong influence of the protein environment on cyclic boronate ester formation.

Influence of the protein environment

The crystal structure of BOS reveals hydrogen bonding interactions between the boronic acid moiety and a neighboring asparagine residue in position 19, spanning the α1 and α4 helices in the 'hinge' region of LmrR giving a striking tightening of the hydrophobic cavity (Figure 4C, RMSD 1.8 Å over all Cα-pairs, SI.23 and SI.24). The N19 residue has a crucial influence on cyclic boronate ester formation, since the catalytically inactive BOS_N19A mutant (which has an otherwise similar ^{11}B NMR spectrum in the absence of ligands) shows a change in equilibrium as well as chemical shifts in the presence of Tris or 4-nitrocatechol (SI.25). The phenyl alanine residue at position 93 appears to be blocking the catalytic boron site and mutation to alanine or glutamic acid increase catalytic activity. A 1.7 Å crystal structure of BOS_EHL was obtained showing an overall similar structure to BOS barring the presence of a molecule of Tris bound at each pBoF residue (Figure 4D, SI.22). While the three mutations do not seem to interact directly with the

boron center, in this structure, dual H-bonding interactions are observed between both the amide and oxygen moieties of the N19 side chain and the boronate ester- and hydroxide moieties.

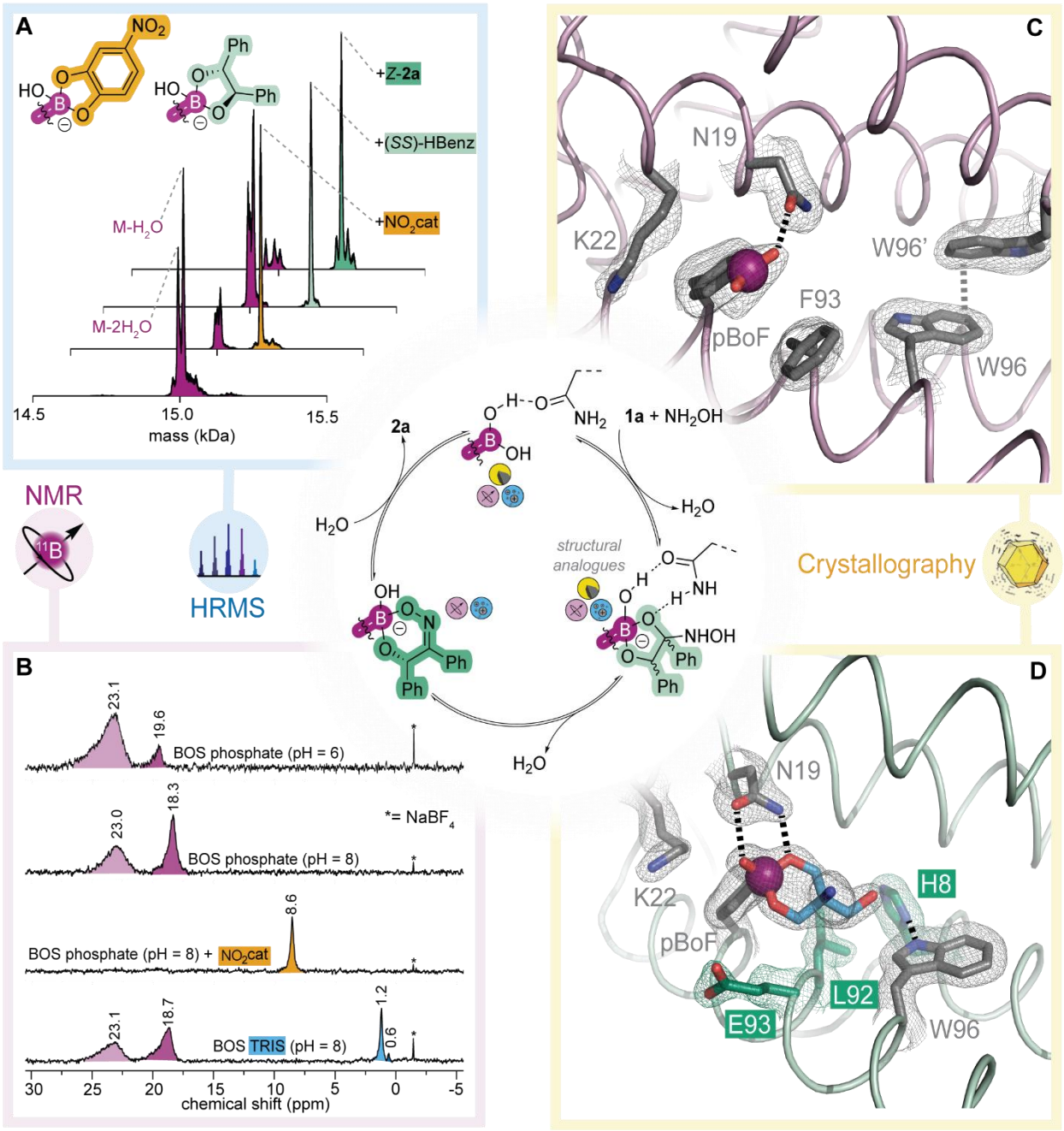

Figure 4. Analysis of the mode of substrate activation and important protein interactions of boronic acid dependent enzyme BOS. **A.** High resolution mass spectrometry of BOS incubated with 4-nitrocatechol, hydrobenzoin and **2a** as evidence for the affinity to diols. **B.** ^{11}B NMR spectroscopic analysis of BOS at different pH (6.0 or 8.0), and the enzyme in the presence of Tris as well as 4-nitrocatechol, IS = $NaBF_4$ (-1.4 ppm). **C.** and **D.** View of the catalytic centers of BOS (PDB: 8QDF) and BOS_EHL (PDB: 8QDH) respectively in their crystal structures with $2F_o$-F_c omit map contoured at 1σ.

The interaction suggests a mechanism where this asparagine stabilizes the key catalytic intermediates via hydrogen bonding which is also supported by molecular docking studies (SI.26).

Combined, these results show how the interplay of a boronic acid catalytic site with a protein scaffold gives rise to a designer enzyme with reactivity that has no precedent in Nature's repertoire. Moreover, this work demonstrates a pathway towards generalizable enantioselective boronic acid catalysis.

Acknowledgements

General: The authors thank J. Kemmink, P. van der Meulen and J. Hekelaar for analytical support. The authors also thank I. Drienovská for the preparation of some of the plasmids used in this work. **Funding**: This work was supported by The Netherlands Ministry of Education, Culture and Science (Gravitation program no. 024.001.035) and the European Research Council (ERC advanced grant 885396). L.L. acknowledges the support of the Leopoldina National Academy of Sciences for a postdoctoral fellowship (LPDS 2021-11). The European Synchrotron Radiation Facility (ESRF) is acknowledged for provision of synchrotron radiation facilities and the authors are grateful to M. Bowler, D. Flot and D. Nurizzo for their assistance and support in using ESRF beamline MASSIF-1. **Authors contributions**: L.L. and R.B.L.G. contributed equally. L.L., R.B.L.G. and G.R. conceived the project. L.L. developed, optimized and performed the scope of the kinetic resolution reaction. R.B.L.G. expressed designer enzymes and performed the evolution campaign. H.J.R. performed crystal growing experiments. A.M.W.H.T. analyzed the X-ray data. G.R. directed the project. All authors discussed the results and L.L., R.B.L.G. and G.R. wrote the manuscript. **Competing interests:** The authors declare no competing interests. **Data and materials availability:** All data are available in the manuscript or the supplementary materials.

List of Supplementary Materials

Materials and Methods (SI.27–SI.33)
Supplementary Text (SI.1–SI.26)
Figs. S1 to S32
Tables S1 to S13
Supporting References

References

1. V. M. Dembitsky, A. A. Al Quntar, M. Srebnik, Natural and Synthetic Small Boron-Containing Molecules as Potential Inhibitors of Bacterial and Fungal Quorum Sensing. *Chem. Rev.* **111**, 209-237 (2011).
2. N. Miyaura, A. Suzuki, Palladium-Catalyzed Cross-Coupling Reactions of Organoboron Compounds. *Chem. Rev.* **95**, 2457-2483 (1995).
3. D. B. Diaz, A. K. Yudin, The versatility of boron in biological target engagement. *Nat. Chem.* **9**, 731-742 (2017).
4. K. Ishihara, H. Yamamoto, Arylboron Compounds as Acid Catalysts in Organic Synthetic Transformations. *Eur. J. Org. Chem.* **1999**, 527-538 (1999).
5. D. G. Hall, Boronic acid catalysis. *Chem. Soc. Rev.* **48**, 3475-3496 (2019).
6. S. Zhang, D. Lebœuf, J. Moran, Brønsted Acid and H-Bond Activation in Boronic Acid Catalysis. *Chem. Eur. J.* **26**, 9883-9888 (2020).
7. B. J. Graham, R. T. Raines, Emergent Organoboron Acid Catalysts. *J. Org. Chem.*, (2022).
8. N. Y. Adonin, V. V. Bardin, Polyfluorinated arylboranes as catalysts in organic synthesis. *Mendeleev Commun.* **30**, 262-272 (2020).
9. K. Ishihara, S. Ohara, H. Yamamoto, 3,4,5-Trifluorobenzeneboronic Acid as an Extremely Active Amidation Catalyst. *J. Org. Chem.* **61**, 4196-4197 (1996).
10. K. Arnold, A. S. Batsanov, B. Davies, A. Whiting, Synthesis, evaluation and application of novel bifunctional N,N-di-isopropylbenzylamineboronic acid catalysts for direct amide formation between carboxylic acids and amines. *Green. Chem.* **10**, 124-134 (2008).
11. R. M. Al-Zoubi, O. Marion, D. G. Hall, Direct and Waste-Free Amidations and Cycloadditions by Organocatalytic Activation of Carboxylic Acids at Room Temperature. *Angew. Chem. Int. Ed.* **47**, 2876-2879 (2008).
12. K.-S. Cao, H.-X. Bian, W.-H. Zheng, Mild arylboronic acid catalyzed selective [4 + 3] cycloadditions: access to cyclohepta[b]benzofurans and cyclohepta[b]indoles. *Org. Biomol. Chem.* **13**, 6449-6452 (2015).
13. H. Zheng, S. Ghanbari, S. Nakamura, D. G. Hall, Boronic Acid Catalysis as a Mild and Versatile Strategy for Direct Carbo- and Heterocyclizations of Free Allylic Alcohols. *Angew. Chem. Int. Ed.* **51**, 6187-6190 (2012).

14. S. Estopiñá-Durán *et al.*, Aryl Boronic Acid Catalysed Dehydrative Substitution of Benzylic Alcohols for C−O Bond Formation. *Chem. Eur. J.* **25**, 3950-3956 (2019).
15. H. H. San, J. Huang, S. Lei Aye, X.-Y. Tang, Boron-Catalyzed Dehydrative Friedel-Crafts Alkylation of Arenes Using β-Hydroxyl Ketone as MVK Precursor. *Adv. Synth. Catal.* **363**, 2386-2391 (2021).
16. N. Hayama, T. Azuma, Y. Kobayashi, Y. Takemoto, Chiral Integrated Catalysts Composed of Bifunctional Thiourea and Arylboronic Acid: Asymmetric Aza-Michael Addition of α,β-Unsaturated Carboxylic Acids. *Chem. Pharm. Bull.* **64**, 704-717 (2016).
17. N. Hayama *et al.*, Mechanistic Insight into Asymmetric Hetero-Michael Addition of α,β-Unsaturated Carboxylic Acids Catalyzed by Multifunctional Thioureas. *J. Am. Chem. Soc.* **140**, 12216-12225 (2018).
18. K. Michigami, H. Murakami, T. Nakamura, N. Hayama, Y. Takemoto, Catalytic asymmetric aza-Michael addition of fumaric monoacids with multifunctional thiourea/boronic acids. *Org. Biomol. Chem.* **17**, 2331-2335 (2019).
19. N. Hayama *et al.*, A solvent-dependent chirality-switchable thia-Michael addition to α,β-unsaturated carboxylic acids using a chiral multifunctional thiourea catalyst. *Chem. Sci.* **11**, 5572-5576 (2020).
20. H. Murakami, A. Yamada, K. Michigami, Y. Takemoto, Novel Aza-Michael Addition-Asymmetric Protonation to α,β-Unsaturated Carboxylic Acids with Chiral Thiourea-Boronic Acid Hybrid Catalysts. *Asian J. Org. Chem.* **10**, 1097-1101 (2021).
21. N. Hayama, Y. Kobayashi, Y. Takemoto, Asymmetric hetero-Michael addition to α,β-unsaturated carboxylic acids using thiourea–boronic acid hybrid catalysts. *Tetrahedron* **89**, 132089 (2021).
22. K. Arnold, B. Davies, D. Hérault, A. Whiting, Asymmetric Direct Amide Synthesis by Kinetic Amine Resolution: A Chiral Bifunctional Aminoboronic Acid Catalyzed Reaction between a Racemic Amine and an Achiral Carboxylic Acid. *Angew. Chem. Int. Ed.* **47**, 2673-2676 (2008).
23. K. Arnold *et al.*, The first example of enamine–Lewis acid cooperative bifunctional catalysis: application to the asymmetric aldol reaction. *Chem. Comm.*, 3879-3881 (2008).
24. I. Georgiou, A. Whiting, Mechanism and optimisation of the homoboroproline bifunctional catalytic asymmetric aldol reaction: Lewis acid tuning through in situ esterification. *Org. Biomol. Chem.* **10**, 2422-2430 (2012).

25. T. Azuma, A. Murata, Y. Kobayashi, T. Inokuma, Y. Takemoto, A Dual Arylboronic Acid–Aminothiourea Catalytic System for the Asymmetric Intramolecular Hetero-Michael Reaction of α,β-Unsaturated Carboxylic Acids. *Org. Lett.* **16**, 4256-4259 (2014).
26. X. Mo, D. G. Hall, Dual Catalysis Using Boronic Acid and Chiral Amine: Acyclic Quaternary Carbons via Enantioselective Alkylation of Branched Aldehydes with Allylic Alcohols. *J. Am. Chem. Soc.* **138**, 10762-10765 (2016).
27. R. B. Leveson-Gower, C. Mayer, G. Roelfes, The importance of catalytic promiscuity for enzyme design and evolution. *Nat. Rev. Chem.* **3**, 687-705 (2019).
28. K. Chen, F. H. Arnold, Engineering new catalytic activities in enzymes. *Nat. Catal.* **3**, 203-213 (2020).
29. E. Brustad *et al.*, A Genetically Encoded Boronate-Containing Amino Acid. *Angew. Chem. Int. Ed.* **47**, 8220-8223 (2008).
30. S. L. Lovelock *et al.*, The road to fully programmable protein catalysis. *Nature* **606**, 49-58 (2022).
31. Z. Birch-Price, C. J. Taylor, M. Ortmayer, A. P. Green, Engineering enzyme activity using an expanded amino acid alphabet. *PEDS* **36**, gzac013 (2023).
32. I. Drienovská, G. Roelfes, Expanding the enzyme universe with genetically encoded unnatural amino acids. *Nat. Catal.* **3**, 193-202 (2020).
33. Z. Zhou, G. Roelfes, Synergistic catalysis in an artificial enzyme by simultaneous action of two abiological catalytic sites. *Nat. Catal.* **3**, 289-294 (2020).
34. A. J. Burke *et al.*, Design and evolution of an enzyme with a non-canonical organocatalytic mechanism. *Nature* **570**, 219-223 (2019).
35. J. S. Trimble *et al.*, A designed photoenzyme for enantioselective [2+2] cycloadditions. *Nature* **611**, 709-714 (2022).
36. N. Sun *et al.*, Enantioselective [2+2]-cycloadditions with triplet photoenzymes. *Nature* **611**, 715-720 (2022).
37. D. O'Hagan, J. W. Schmidberger, Enzymes that catalyse SN2 reaction mechanisms. *Nat. Prod. Rep.* **27**, 900-918 (2010).
38. M. Gabruk, B. Mysliwa-Kurdziel, Light-Dependent Protochlorophyllide Oxidoreductase: Phylogeny, Regulation, and Catalytic Properties. *Biochemistry* **54**, 5255-5262 (2015).
39. D. Sorigué *et al.*, Mechanism and dynamics of fatty acid photodecarboxylase. *Science* **372**, eabd5687 (2021).

40. H. Agustiandari, J. Lubelski, H. B. v. d. B. v. Saparoea, O. P. Kuipers, A. J. M. Driessen, LmrR Is a Transcriptional Repressor of Expression of the Multidrug ABC Transporter LmrCD in Lactococcus lactis. *J. Bacteriol.* **190**, 759-763 (2008).
41. G. Roelfes, LmrR: A Privileged Scaffold for Artificial Metalloenzymes. *Acc. Chem. Res.* **52**, 545-556 (2019).
42. E. L. Simionatto, P. R. Yunes, R. A. Yunes, The effect of boric acid on the dehydration step in the formation of oxime from salicylaldehyde. *J. Chem. Soc., Perkin trans. 2*, 1291-1294 (1993).
43. T. C. Bhalla, V. Kumar, V. Kumar, Enzymes of aldoxime–nitrile pathway for organic synthesis. *Rev. Environ. Sci. Biotechnol.* **17**, 229-239 (2018).
44. N. Hiroaki, O. Tadashi, F. Takayuki, Hydrolysis of N-Salicylidene-2-methoxyethylamine. Intramolecular General Base Catalysis and Specific Effects of Boric Acid. *Bull. Chem. Soc. Jpn.* **57**, 2502-2507 (1984).
45. D. Gillingham, The role of boronic acids in accelerating condensation reactions of α-effect amines with carbonyls. *Org. Biomol. Chem.* **14**, 7606-7609 (2016).
46. P. K. Madoori, H. Agustiandari, A. J. M. Driessen, A.-M. W. H. Thunnissen, Structure of the transcriptional regulator LmrR and its mechanism of multidrug recognition. *EMBO J.* **28**, 156-166 (2009).
47. K. Faber, in *Biotransformations in Organic Chemistry: A Textbook*. (Springer Berlin Heidelberg, Berlin, Heidelberg, 2011), pp. 31-313.
48. R. H. de Vries, J. H. Viel, O. P. Kuipers, G. Roelfes, Rapid and Selective Chemical Editing of Ribosomally Synthesized and Post-Translationally Modified Peptides (RiPPs) via CuII-Catalyzed β-Borylation of Dehydroamino Acids. *Angew. Chem. Int. Ed.* **60**, 3946-3950 (2021).
49. E. Tsilikounas, C. A. Kettner, W. W. Bachovchin, Boron-11 NMR spectroscopy of peptide boronic acid inhibitor complexes of .alpha.-lytic protease. Direct evidence for tetrahedral boron in both boron-histidine and boron-serine adduct complexes. *Biochemistry* **32**, 12651-12655 (1993).
50. J. M. Macho, R. M. Blue, H.-W. Lee, J. B. MacMillan, Boron NMR as a Method to Screen Natural Product Libraries for B-Containing Compounds. *Org. Lett.* **24**, 3161-3166 (2022).

51. S. A. Valenzuela, J. R. Howard, H. M. Park, S. Darbha, E. V. Anslyn, 11B NMR Spectroscopy: Structural Analysis of the Acidity and Reactivity of Phenyl Boronic Acid–Diol Condensations. *J. Org. Chem.* **87**, 15071-15076 (2022).

52. D. N. Barsoum, V. C. Kirinda, B. Kang, J. A. Kalow, Remote-Controlled Exchange Rates by Photoswitchable Internal Catalysis of Dynamic Covalent Bonds. *J. Am. Chem. Soc.* **144**, 10168-10173 (2022).